

Research Article

Determination and Analysis of Radiation Shielding Properties of Some Selected Building Materials

Elisha Daniel Edmund^{1,2,*}, Joseph Amoako^{1,3}, Philip Deatanyah^{1,3},
Machibya Matulanya²

¹Graduate School of Nuclear and Allied Sciences, University of Ghana-Atomic Campus, Accra, Ghana

²Tanzania Atomic Energy Commission (TAEC), Dodoma, Tanzania

³Radiation Protection Institute, Ghana Atomic Energy Commission, Accra, Ghana

Abstract

Background: Radiation shielding primarily is based on the principle of attenuation of beams of X-ray or gamma radiation by absorption or scattering of the radiation that results due to the interaction between penetrating radiation and matter, radiation shielding properties such as attenuation coefficients obtained as a result of interaction between X-rays and gamma rays with target materials helps to study and confirm the appropriate building materials used for radiation shielding purposes. The linear attenuation coefficient required by radiation engineers in the design and analysis of radiation facilities has been determined and analysed for both gamma ray source Cs-137 and X-ray sources for 662 keV and 60- 120 kVp respectively. **Methods:** The determination of linear attenuation coefficient was evaluated by the formulation of building materials such as lead, granite, aluminium and concrete by calculating and comparing both experimental and theoretical results for 662 keV and 60-120 kVp using collimated Source-Material-Detector geometry method and XCOM software respectively. **Conclusion:** The results agreed with similar experimental works and the use of XCOM software with a percentage deviation of 0.44% - 11% at the 95 % confidence level. It was concluded that the results will go in a long way in assisting engineers and radiation professionals in the design and protection of radiation facilities.

Keywords

Linear Attenuation, X-rays, Gamma Ray, XCOM

1. Introduction

Electromagnetic radiations associated with high frequencies such as X and Gamma rays play a significant role to provide necessary informations for both medical and non-medical applications hence save thousands of lives each year throughout the world. When radiation interacts with any material, its intensity gradually reduces as a result, the prob-

ability of radiation interacting with a material per unit path length was defined by Wood as far back as 1982 [1]. This property, the linear attenuation coefficient of the material is an important quantity used in characterizing the penetration and diffusion of radiation in the medium. An important component of radiation safety programs aims at reducing personnel

*Corresponding author: edmundelisha511@yahoo.com (Elisha Daniel Edmund)

Received: 22 December 2023; **Accepted:** 18 January 2024; **Published:** 2 April 2024



Copyright: © The Author(s), 2024. Published by Science Publishing Group. This is an **Open Access** article, distributed under the terms of the Creative Commons Attribution 4.0 License (<http://creativecommons.org/licenses/by/4.0/>), which permits unrestricted use, distribution and reproduction in any medium, provided the original work is properly cited.

exposure to ionizing radiation through radiation attenuation. Attenuation data for most commonly used shielding materials have been published and are available in many resources, such as the NIST. WINXCOM database of attenuation coefficient, dosimetry, agriculture, industry, health physics and radiological health [2, 14]. A computer program WINXCOM, developed by Berger and Hubbell calculates photon cross-sections and attenuation coefficient for pure elements and mixtures in the energy range of 1 keV to 100 GeV. Recently, several pieces of research have been conducted on the determination of attenuation coefficient, both theoretically and experimentally for different materials. This mostly depends on the photon energy, the nature of the material and the density of the medium [3-7, 16].

Despite there are several studies have been conducted on radiation shielding and shielding materials, there is still a need to find effective construction materials which can give adequate shielding capabilities while taking into consideration the cost-effectiveness since most materials are expensive and not available locally.

The main objectives of this current work is to formulate and experimentally determine the linear attenuation coefficient of Aluminium, Concrete, Lead and Granite. Specifically fabri-

cate species of concrete based on mixing ratios, determine and estimate mass attenuation coefficients, half-value layer, mean free path, tenth value layer, and density of selected building materials using varied energies of X-ray and Gamma-ray sources, compare the current results to other similar results and standards.

2. Materials and Methods

The materials used for the fabrication were mostly local building materials from various districts within the Greater Accra region of Ghana. These were sand, quarry-dusts, Portland cement (Diamond cement), Aluminium, Lead and Granite.

The materials used for the study were prepared at Ghana Atomic Energy Commission (GAEC) mechanical workshop and moulded into rectangular slabs of 100 mm by 100 mm dimensions. The thickness of materials varied, (1.5 - 4.5) mm of Lead, (20-60) mm for Granite and (6-10) mm of Aluminium for transmission experiment. Three different series of concretes were fabricated experimentally using ratios of Quarry dust, sand, Ordinary Portland cement (Diamond Cement) and water as indicated in table 1.

Table 1. Different concrete mixtures with their respective designed codes: C1, C2 and C3.

CONCRETE CODE	QUARRY DUST (g)	CEMENT (g)	RIVER SAND (g)	WATER (g)	W/C RATIO	MIXING RATIO
CSQW (C1)	800	100	400	90	0.90	1:4:8
CQW (C2)	0	800	2400	549.6	0.69	1:3
CSW (C3)	2100	700	0	500	0.71	1:3

These materials were dried in an oven for 24 hours and sieved into powder form at an Environmental laboratory of the Radiation Protection Institute (RPI). Concrete mixtures with different codes C1, C2 and C3, and prepared with specifications of Indian Bureau of Standard (IS 456:2000) as shown in table 1 and moulded with the dimensions of (100 mm x 100 mm) and thicknesses of (20-50) mm. The curing process by watering concrete was done for 28 days while drying the concretes in the sun.

2.1. Cs-137 Irradiation

A narrow-collimated beam of Cesium-137 with the energy of 662 keV installed in the Secondary Standard Dosimetry Laboratory (SSDL) of the Radiation Protection Institute (RPI) and a calibrated Survey meter, used as a

detector for the experimental irradiation process. All measurements during the irradiations of the building materials were taken at approximately possible to standard conditions of temperature and pressure (STP). The detector system used was a calibrated Survey meter CANBERRA-RADIAGEM, with a model RAD 2000 and a serial number of 4557. The sensitivity range was 0.3 μ Sv/hr - 100 mSv/hr. The central horizontal head of the survey meter was aligned to the source using a laser alignment system with the help of the calibration bench at a fixed distance of 100 cm from the focal point of the Cs-137 sources as indicated in figure 1. The setup was designed such that the source of radiation and detector system is on the same level. Different construction materials under investigation with varying thickness were placed at a distance of 50 cm from the radiation source and survey meter for transmission irradiation tests.

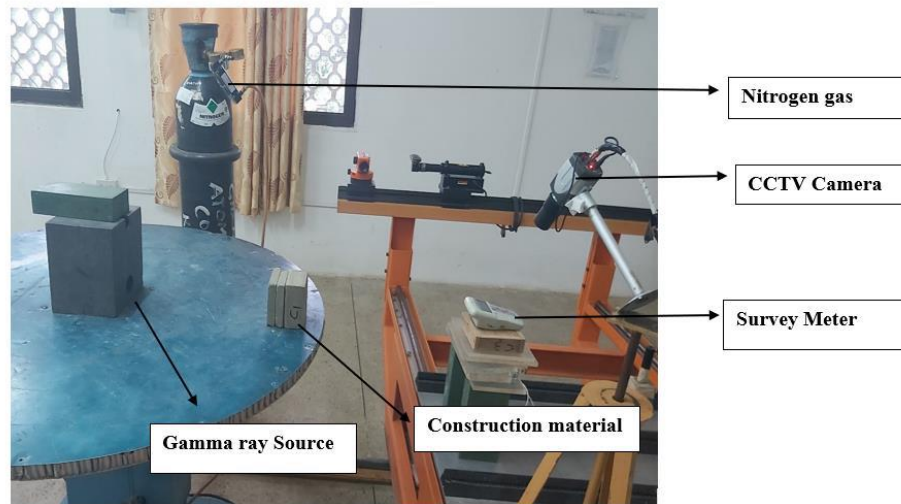


Figure 1. Construction material placed between Gamma-ray source and detector.

The irradiation was carried on in two steps: One with the material in place and the second without the material in place for 20 seconds each respectively. The procedure was repeated for different varied construction material of various thicknesses. To reduce the statistical error, the measurements for each type of material sample for a given thickness was repeated 10 times, for the accuracy of the measurements the average values and standard deviations for the readings were computed.

2.2. X-Ray Irradiation

The use of an X-ray facility was carried out at the University of Ghana Hospital. The UNIVERSAL DELFI General X-ray machine with a model collimator type R302 F/A and a serial number R 302/A DHHS was used. The peak voltage ranges from (40 - 150) kVp and maximum current of 200 mA. A calibrated PTW NOMEX Multimeter manufactured by PTW-Freiburg, Germany reference number T11049 and serial

number 101758 was used for exposure measurements.

To assure consistency of the performance of the x-ray machine, the following quality assurance task was performed. These were: kVp accuracy test, Reproducibility test and Linearity test. The Nomex meter was placed on the couch at 100 cm, source to detector distance from the X-ray machine. From the console of the x-ray machine in the control room, exposure of x-rays was carried out at tube voltage of (60, 80, 100 120) kVp, tube current of 200 mA and exposure time of 50 ms, and without any construction material between the source and Nomex Multimeter to record the initial readings of exposures. Five readings were taken to reduce the statistical errors between parameters using Nomex software, the reading of parameters such as dose, dose rate, kVp, exposure time and half-value layer were recorded on the datasheet. The different construction material of varying thicknesses was then placed between the x-ray source and the detector at the distance of 5 cm from the detector as indicated in figure 2.

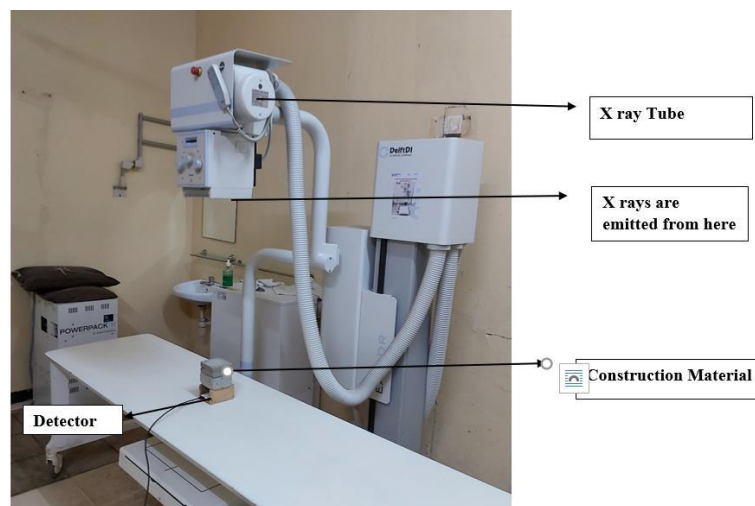


Figure 2. Construction material placed between the X-ray source and Nomex Multimeter detector.

Exposures were carried out five times for each thickness of construction material with energies ranging from (60-120) kVp and the parameters were recorded by using Nomex software installed at the computer.

The density of all materials was assessed by measuring the mass using a calibrated electronic weighing device. The volume of each material was determined from the product of the length, width and height by the use of the Vernier caliper. The density was then estimated using equation 1:

$$\rho = \frac{m}{v} \quad (1)$$

Where ρ is the density of materials, m is the mass of the materials in g, and v is the volume of the materials in cm

The linear attenuation coefficients were estimated by employing the Beer-Lambert law as a result of interaction between incident photons and shielding materials (absorbers) by comparing I_0 and I which are incident and attenuated quantities (dose rates) with and without the absorber thickness x (cm) as shown in equation 2:

$$I(x) = I_0 e^{-\mu x} \quad (2)$$

where the μ (cm^{-1}) represents the linear attenuation coefficient of the absorber. The mass attenuation coefficient was estimated using equation 3:

$$\mu_m = \frac{\mu}{\rho} \quad (3)$$

Where μ_m (cm^2g^{-1}) represents the mass attenuation coefficient. The average distance at which a single photon travels through the medium of a given material before interacting with materials, the mean free path was estimated as the inverse of the linear attenuation coefficient.

Furthermore, the halve and tenth value layers in centimeters were respectively estimated using equations 4 and 5:

$$HVL = \frac{0.693}{\mu} \quad (4)$$

$$TVL = \frac{2.303}{\mu} \quad (5)$$

The uncertainties associated with each measured value was based solely on statistical sources. The mean values of measurement and associated standard error of the mean were estimated using R-statistical software [7].

Table 2. kVp Accuracy.

kVp	kVp Average	% Error	Pass/Fail
60	60.9	1.5	Pass
70	71.0	1.4	Pass
80	80.6	0.7	Pass
90	90.8	0.9	Pass
100	100.6	0.6	Pass
120	120.3	0.2	Pass

Table 3. Reproducibility test.

	kVp Average	Time (msec)	Dose (μGy)
	80.6	50.5	239.5
	80.6	50.0	239.8
	80.3	50.5	241.0
	80.6	51.0	240.1
	80.7	51.0	239.2
	81.1	51.0	240.2
Average	80.66	50.67	239.9667
CV	0.0032	0.0081	0.0026
P/F	Pass	Pass	Pass

Table 4. mAs Linearity test.

mAs	Dose (μGy)	$\mu\text{Gy/mAs}$	CV	P/F
4	270.6	67.650	-	-
8	545.2	68.150	0.004	Pass
16	1027	64.188	0.030	Pass
32	2047	63.968	0.002	Pass
64	4085	63.828	0.001	Pass
125	8200.6	65.605	0.014	Pass

3. Results and Discussions

Tables 2 and 4 shows the results of quality control tests performed on the General Radiography X-ray machine to verify that the machine was working properly and consistently. The results show a good agreement and consistent with the standard.

Figure 3 shows the results of plots of material thickness and the natural logarithm of the ratio of the final and initial radiation source intensity of the various materials at the 95 % confidence level using a linear modelling approach. The results in general showed an inverse relationship with the source energy. However, each linear attenuation coefficient derived from the slope

exhibited a unique characteristic of the material.

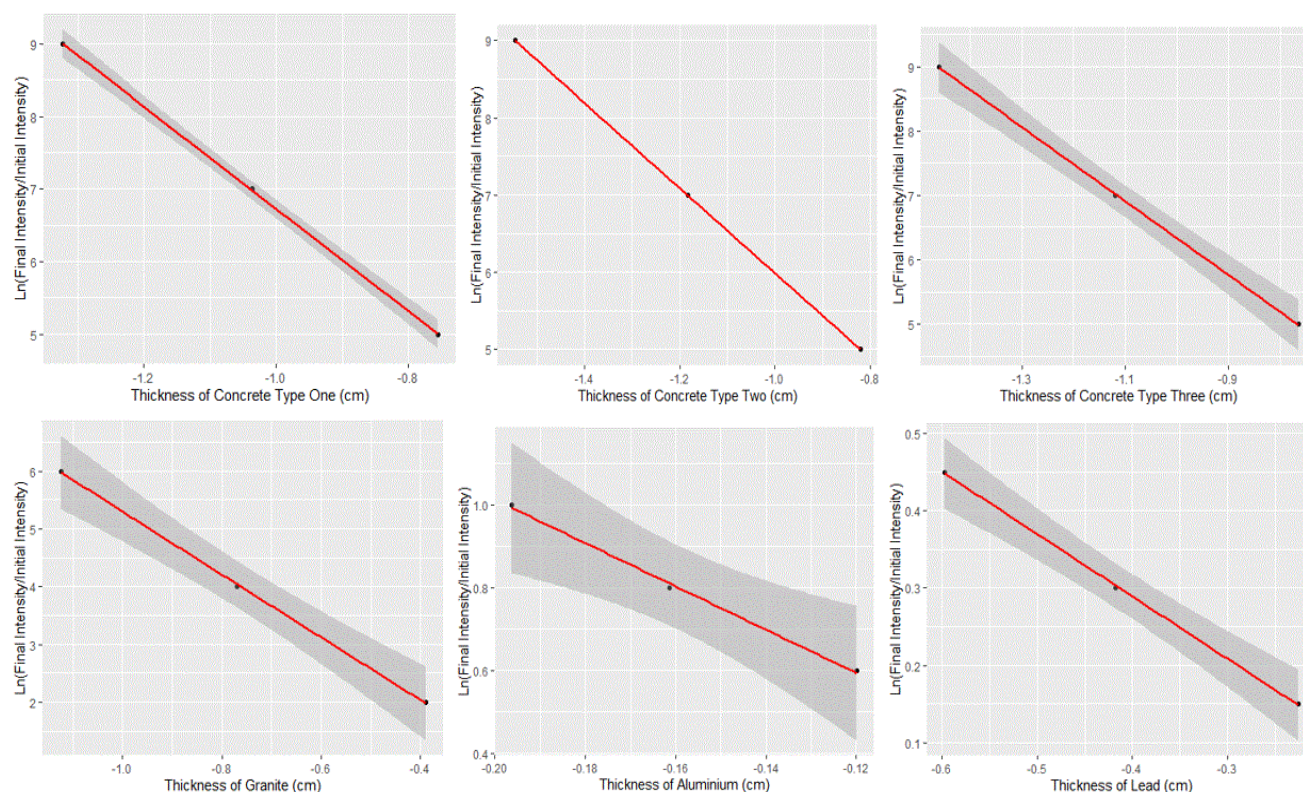


Figure 3. Determination of linear attenuation factors of selected materials using a linear modelling technique.

This uniqueness of each material is inherent in the corresponding linear attenuation coefficient as a result. This characteristic is summarized in tables 5, 6, 7, 8 and 9. The mass attenuation coefficient exhibited characteristics similar to the linear attenuation coefficient with an influence on the density

of each material. The half-value (HVL) and tenth value layers (TVL) are quantities that describe the interaction of x rays and gamma radiations with the shielding materials, they are very useful to engineers in fulfilling the requirements of radiation protection of facilities.

Table 5. Shielding properties and associated standard errors of the various construction materials using cesium-137 source.

Sample	Thickness (mm)	Density (g/cm ³)	Linear attenuation μ (cm ⁻¹)	Mass attenuation μ_m (cm ² /g)	Half value layer (cm)	Tenth value (cm)	Mean free path (cm)
Lead	1.5	11.3612	1.5026 ± 0.058	0.1323 ± 0.0051	0.4613	1.5324	0.6655
	3.0		1.3911 ± 0.033	0.1224 ± 0.0029	0.4983	1.6555	0.7189
	4.5		1.3273 ± 0.025	0.1168 ± 0.0022	0.5222	1.7348	0.7534
	6		0.1998 ± 0.005	0.0735 ± 0.0020	3.4692	11.5244	5.0050
Aluminium	8	2.7189	0.2016 ± 0.003	0.0741 ± 0.0014	3.4382	11.4216	4.9603
	10		0.1962 ± 0.003	0.0722 ± 0.0014	3.5329	11.7359	5.0968
	20		0.1952 ± 0.0029	0.0735 ± 0.0018	3.5510	11.7960	5.1230
Granite	40	2.6567	0.1924 ± 0.0036	0.0724 ± 0.0019	3.6026	11.9677	5.1976
	60		0.1874 ± 0.0032	0.0705 ± 0.0018	3.6988	12.2870	5.3362
Concrete (C1)	50	2.0248	0.1513 ± 0.0027	0.0747 ± 0.0019	4.5813	15.2187	6.6094

Sample	Thickness (mm)	Density (g/cm ³)	Linear attenuation μ (cm ⁻¹)	Mass attenuation μ_m (cm ² /g)	Half value layer (cm)	Tenth value (cm)	Mean free path (cm)
Concrete (C2)	70	2.3260	0.1481 \pm 0.0021	0.0731 \pm 0.0017	4.6803	15.5475	6.7522
	90		0.1470 \pm 0.0033	0.0726 \pm 0.0021	4.7153	15.6638	6.8027
	50		0.1642 \pm 0.0026	0.0706 \pm 0.0012	4.2214	14.0231	6.0901
	70		0.1691 \pm 0.0025	0.0727 \pm 0.0012	4.0990	13.6167	5.9137
	90		0.1717 \pm 0.0034	0.0738 \pm 0.0015	4.0370	13.4105	5.8241
	50		0.1531 \pm 0.0025	0.0739 \pm 0.0018	4.5274	15.0397	6.5317
Concrete (C3)	70	2.0724	0.1600 \pm 0.0029	0.0772 \pm 0.0015	4.3322	14.3912	6.2500
	90		0.1623 \pm 0.0044	0.0783 \pm 0.0022	4.2708	14.1872	6.1614

Table 6. Shielding properties and associated standard errors of the various construction materials using X-ray source at 60 kVp.

Sample	Thickness (mm)	Density (g/cm ³)	Linear attenuation μ (cm ⁻¹)	Mass Attenuation μ_m (cm ² /g)	Half Value Layer (cm)	Tenth Value Layer (cm)	Mean Free Path (cm)
Granite	20	2.6567	1.6076 \pm 0.0064	0.6051 \pm 0.012	0.4312	1.4323	0.6220
	40		1.3267 \pm 0.022	0.4994 \pm 0.013	0.5225	1.7356	0.7537
	60		0.9521 \pm 0.015	0.3584 \pm 0.0087	0.7280	2.4184	1.0503
Aluminum	6	2.7189	2.1017 \pm 0.020	0.7730 \pm 0.011	0.3298	1.0956	0.4758
	8		1.9603 \pm 0.016	0.7210 \pm 0.0099	0.3536	1.1746	0.5101
	10		1.8604 \pm 0.017	0.6842 \pm 0.0098	0.3726	1.2377	0.5375
Concrete (C1)	20	2.0248	1.3566 \pm 0.0059	0.6670 \pm 0.013	0.5109	1.6973	0.7371
	40		1.1345 \pm 0.0063	0.5603 \pm 0.011	0.6110	2.0296	0.8814
	50		1.0514 \pm 0.0044	0.5193 \pm 0.010	0.6593	2.1900	0.9511
Concrete (C2)	20	2.3260	1.5628 \pm 0.0048	0.6719 \pm 0.006	0.4435	1.4734	0.6399
	40		1.3164 \pm 0.0098	0.5659 \pm 0.0064	0.5265	1.7492	0.7596
	50		1.1263 \pm 0.0287	0.4842 \pm 0.013	0.6154	2.0444	0.8879
Concrete (C3)	20	2.0724	1.7057 \pm 0.011	0.8231 \pm 0.013	0.4064	1.3499	0.5863
	40		1.3955 \pm 0.039	0.6734 \pm 0.021	0.4967	1.6500	0.7166
	50		1.1722 \pm 0.018	0.5656 \pm 0.012	0.5913	1.9643	0.8531

Table 7. Shielding properties and associated standard errors of the various construction materials using X-ray source at 80 kVp.

Sample	Thickness (mm)	Density (g/cm ³)	Linear attenuation μ (cm ⁻¹)	Mass Attenuation μ_m (cm ² /g)	Half Value Layer (cm)	Tenth Value Layer (cm)	Mean Free Path (cm)
Granite	20	2.6567	1.2219 \pm 0.0037	0.4599 \pm 0.0087	0.5673	1.8844	0.8184
	40		0.9949 \pm 0.011	0.3745 \pm 0.0081	0.6967	2.3144	1.0051
	60		0.8878 \pm 0.012	0.3342 \pm 0.0077	0.7807	2.5936	1.1264
Aluminum	6	2.7189	1.6983 \pm 0.014	0.6246 \pm 0.0086	0.4081	1.3558	0.5888
	8		1.5686 \pm 0.0098	0.5769 \pm 0.0073	0.4419	1.4679	0.6375

Sample	Thickness (mm)	Density (g/cm ³)	Linear attenuation μ (cm ⁻¹)	Mass Attenuation μ_m (cm ² /g)	Half Value Layer (cm)	Tenth Value Layer (cm)	Mean Free Path (cm)
Concrete (C1)	10	2.0248	1.4759 \pm 0.0074	0.5428 \pm 0.0065	0.4696	1.5601	0.6776
	20		1.0587 \pm 0.0027	0.5229 \pm 0.010	0.6547	2.1749	0.9446
	40		0.8467 \pm 0.0083	0.4182 \pm 0.0092	0.8186	2.7195	1.1811
	50		0.7789 \pm 0.0089	0.3847 \pm 0.0087	0.8899	2.9562	1.2839
Concrete (C2)	20	2.3260	1.1913 \pm 0.0038	0.5122 \pm 0.0046	0.5818	1.9328	0.8394
	40		0.9896 \pm 0.0062	0.4255 \pm 0.0045	0.7004	2.3268	1.0105
	50		0.8434 \pm 0.0065	0.3626 \pm 0.0041	0.8218	2.7301	1.1857
Concrete (C3)	20	2.0724	1.2718 \pm 0.0049	0.6137 \pm 0.0091	1.8105	1.8105	0.7863
	40		1.0267 \pm 0.0061	0.4954 \pm 0.0077	0.6751	2.2427	0.9740
	50		0.8539 \pm 0.0069	0.4120 \pm 0.0068	0.8117	2.6966	1.1711

Table 8. Shielding properties and associated standard errors of the various construction materials using X-ray source at 100 kVp.

Sample	Thickness (mm)	Density (g/cm ³)	Linear attenuation μ (cm ⁻¹)	Mass Attenuation μ_m (cm ² /g)	Half Value Layer (cm)	Tenth Value Layer (cm)	Mean Free Path (cm)
Granite	20	2.6567	1.0022 \pm 0.0031	0.3772 \pm 0.0071	0.6916	2.2975	0.9978
	40		0.8275 \pm 0.0012	0.3115 \pm 0.0058	0.8376	2.7826	1.2085
	60		0.7578 \pm 0.0037	0.2852 \pm 0.0055	0.9147	3.0385	1.3196
Aluminum	6	2.7189	1.3976 \pm 0.012	0.5140 \pm 0.0071	0.4960	1.6475	0.7155
	8		1.2906 \pm 0.0081	0.4747 \pm 0.0060	0.5371	1.7841	0.7748
	10		1.2164 \pm 0.0061	0.4474 \pm 0.0054	0.5698	1.8930	0.8221
Concrete (C1)	20	2.0248	0.8586 \pm 0.0023	0.4240 \pm 0.0084	0.8073	2.6818	1.1647
	40		0.7043 \pm 0.0023	0.3478 \pm 0.0069	0.9842	3.2693	1.4198
	50		0.6449 \pm 0.0021	0.3185 \pm 0.0063	1.0748	3.5705	1.5506
Concrete (C2)	20	2.3260	1.0261 \pm 0.0026	0.4411 \pm 0.0039	0.6755	2.2440	0.9746
	40		0.8225 \pm 0.0031	0.3536 \pm 0.0033	0.8427	2.7995	1.2158
	50		0.6931 \pm 0.0036	0.2980 \pm 0.0029	1.0001	3.3222	1.4428
Concrete (C3)	20	2.0724	1.0186 \pm 0.0029	0.4915 \pm 0.0072	0.6805	2.2605	0.9817
	40		0.8395 \pm 0.0015	0.4051 \pm 0.0059	0.8257	2.7428	1.1912
	50		0.7094 \pm 0.0032	0.3423 \pm 0.0051	0.9771	3.2458	1.4096

Table 9. Shielding properties and associated standard errors of the various construction materials using X-ray source at 120 kVp.

Sample	Thickness (mm)	Density (g/cm ³)	Linear attenuation μ (cm ⁻¹)	Mass Attenuation μ_m (cm ² /g)	Half Value Layer (cm)	Tenth Value Layer (cm)	Mean Free Path (cm)
Granite	20	2.6567	0.9382 \pm 0.002	0.3531 \pm 0.0066	0.7388	2.4543	1.0659
	40		0.7393 \pm 0.0013	0.2783 \pm 0.0053	0.9376	3.1145	1.3526
	60		0.6569 \pm 0.0017	0.2473 \pm 0.0047	1.0552	3.5052	1.5223

Sample	Thickness (mm)	Density (g/cm ³)	Linear attenuation μ (cm ⁻¹)	Mass Attenuation μ_m (cm ² /g)	Half Value Layer (cm)	Tenth Value Layer (cm)	Mean Free Path (cm)
Aluminium	6	2.7189	1.2033 \pm 0.001	0.4426 \pm 0.0049	0.5760	1.9136	0.8310
	8		1.1114 \pm 0.006	0.4088 \pm 0.0050	0.6237	2.0718	0.8998
	10		1.0471 \pm 0.005	0.3851 \pm 0.0048	0.6620	2.1990	0.9550
Concrete (C1)	20	2.0248	0.7647 \pm 0.0019	0.3777 \pm 0.0075	0.9064	3.0111	1.3077
	40		0.6184 \pm 0.00077	0.3054 \pm 0.0060	1.1209	3.7235	1.6171
	50		0.5596 \pm 0.00066	0.2764 \pm 0.0055	1.2386	4.1147	1.7870
Concrete (C2)	20	2.3260	0.8581 \pm 0.0021	0.3689 \pm 0.0033	0.8078	2.6834	1.1654
	40		0.7152 \pm 0.00091	0.3075 \pm 0.0027	0.9692	3.2195	1.3982
	50		0.6050 \pm 0.00069	0.2601 \pm 0.0023	1.1457	3.8059	1.6529
Concrete (C3)	20	2.0724	0.8882 \pm 0.0022	0.4286 \pm 0.0063	0.7804	2.5924	1.1259
	40		0.7330 \pm 0.00095	0.3537 \pm 0.0051	0.9456	3.1413	1.3643
	50		0.6134 \pm 0.00067	0.2960 \pm 0.0043	1.1300	3.7538	1.6303

Mean free path (MFP) is the average distance a photon traverses between collisions. The range of a single photon in matter cannot be predicted, thus the average distance travelled before a collision can be calculated from the measured values of linear attenuation coefficients of all construction materials. It can be observed from [table 5](#) that low energy photons can lose its energy in a short distance while high energy photon needs long distance to lose its energy, this implies low energy of photons have lower mean free path and high energy photons have a higher mean free path. It can also be seen that each construction material has its mean free path, this is due to its dependence on linear attenuation coefficient and it's known that the linear attenuation depends on the elemental or

chemical composition of construction material and the energy of the incident photon.

Comparing the results of this current work with a simulation using XCOM program version 3.1 [\[8\]](#) yielded a good agreement with a maximum deviation of 11 %. This is indicated in [table 10](#).

The percentage deviations (PD) of attenuation coefficients among the measured and theoretical was computed with the use of following relation [\[16\]](#).

$$PD = \left(\frac{\mu_{\text{exp}} - \mu_{\text{theory}}}{\mu_{\text{exp}}} \right) \times 100\% \quad (6)$$

Table 10. Experimental and Theoretical Linear Attenuation Coefficients (cm⁻¹).

Construction Material	Experiment	Theory	% Deviation
Lead	1.4070 \pm 3.86E-2	1.2507	11.11
Aluminium	0.1989 \pm 3.66E-3	0.2015	1.30
Granite	0.1917 \pm 3.23E-3	0.2047	6.78
Concrete (C1)	0.1488 \pm 2.70E-3	0.1553	3.86
Concrete (C2)	0.1683 \pm 2.83E-3	0.1773	5.34
Concrete (C3)	0.1585 \pm 3.26E-3	0.1592	0.44

Comparing this current work to similarly published works elsewhere showed a good agreement.

Table 11. Shows a summary of the results.

Material	Exp This study	XCOM This Study	Exp [15]	XCOM [11]
Granite	0.0721	0.0769	0.074	0.0767
	Exp This Study	XCOM This Study	Exp [4]	XCOM [12]
Lead	0.1175	0.1101	0.1179	0.1101
	Exp This study	XCOM This study	Exp [9]	XCOM [13]
Concrete	0.0765	0.0769	0.082	0.078
	Exp This Study	XCOM This Study	Exp [10]	XCOM [10]
Aluminum	0.0733	0.07466	0.073	0.074

The variation in the results could be as a result of varied thicknesses employed and variation in formulated densities of some of the materials due to mixing ratios and elemental compositions such as concrete. Materials such as granite and concrete may also be affected by elemental compositions. Furthermore, inconsistencies in the experimental setups and detector geometries could also contribute to the variations in the results.

4. Conclusion

The process of design and selection of efficient construction material for radiation shielding requires proper study of all shielding properties. The linear attenuation coefficient a variation of Concrete, Granite, Lead and aluminium, required by radiation shielding engineers to design facilities has been determined. The results showed a good agreement with a maximum deviation of 11 % at the 95 % confidence level when compared to other similar works elsewhere. Even though the results agreed, there was some variation due to formulations and uncertainties associated with the work.

Acknowledgments

The authors gratefully acknowledge the management of Radiation Protection Institute of the Ghana Atomic Energy Commission and the Department of Medical Physics, Graduate School of Nuclear and Allied Sciences, Legon, Ghana for their assistance to use equipments and facilities during the collection of data. This work was supported by funding from International Atomic Energy Commission (IAEA) through AFRA-NEST programme.

Conflicts of Interest

The authors declare no conflict of interest.

References

- [1] Robert, E. K.; The history and use of our earth's chemical elements. A reference guide 2nd ed, July 30, 2006.
- [2] Ragheb, M. Radiation Physics 3rd ed. John Wiley and Sons, 2007.
- [3] NIST-National Institute of Standards and Technology. X-ray mass attenuation coefficients, 2013.
- [4] Hubbell, J. H; Seltzer S. M.; Tables of X-Ray of Mass attenuation coefficient and mass-energy absorption coefficient 1 KeV to 20 MeV for elements Z=1 to 92 and 48 additional substances of dosimetric interest, 1995.
- [5] Vandana, A. T.; Pawar, P. P.; Shengule, D. R.; Jadhav, K. M.; Gamma Ray Photon Interaction Studies of Zn in the Energy Range 360 - 1330keV photons. J App Sci India 4, p. 2191-2196, 2012.
- [6] Shultis, J. K.; Faw, R. E. Radiation shielding technology. Health Physics, 88(4), p. 297–322, 2005. Available at: <https://doi.org/10.1097/01.HP.0000148615.73825.b1>
- [7] Rstudio Team.; RSTUDIO.; Integrated Development Environment for R. Rstudio, PBC, Boston, MA URL, 2021. Available at: <http://www.rstudio.com/>
- [8] Tekin, H. O.; Erguzel, T. T.; Sayyed, M. I.; Singh, V. P.; Manici, T.; Altunsoy, E. E.; Agar, O. An investigation on shielding properties of different granite samples using MCNPX code. Digest Journal of Nanomaterials and Biostructures, 13(2), p. 381-389, 2018.
- [9] Georgieva, S.; Barandovski, L. Measurement of the mass attenuation coefficient from 81 keV to 1333 keV for elemental materials Al, Cu and Pb. AIP Conference Proceedings, p. 7–10, 2016. Available at: <https://doi.org/10.1063/1.4944211>
- [10] Demir, N.; Tarim, U. A.; Popovici, M. A.; Demirci, Z. N.; Gurler, O.; Akkurt, I. Investigation of mass attenuation coefficients of water, concrete and bakelite at different energies using the FLUKA Monte Carlo code. Journal of Radioanalytical and Nuclear Chemistry, 298(2), p. 1303–1307, 2013. Available at: <https://doi.org/10.1007/s10967-013-2494-y>

- [11] Pawar, P. P. Measurement of mass and linear attenuation coefficients of gamma-rays of Al for 514, 662 and 1280 keV photons. *Journal of Chemical and Pharmaceutical Research*, 3(4), p. 899-903, 2011.
- [12] Gerward, L.; Guilbert, N.; Jensen, K. B.; Leving, H. WinX-COM - A program for calculating X-ray attenuation coefficients. *Radiation Physics and Chemistry*, 2004. Available at: <https://doi.org/10.1016/j.radphyschem.2004.04.040>
- [13] Najam, L. A.; Hashim, A. K.; Ahmed, H. A.; Hassan, I. M. Study the Attenuation Coefficient of Granite to Use It as Shields against Gamma Ray. *Scientific Research Publishing*, 04(02), p. 33-39, 2016. Available at: <https://doi.org/10.4236/detection.2016.42005>
- [14] Gökçe, H. S. Experimental and Theoretical (XCOM) Calculation Techniques for Gamma-Ray Attenuation Characteristics of Concrete Shields. 3rd International Conference on Advanced Engineering Technologies, 2019.
- [15] Osman, O. Calculation of gamma ray attenuation coefficients of some granite samples using a Monte Carlo simulation code. *Journal of Radiation Physics and Chemistry*, (144), p. 271-275, 2018.
- [16] Agar, O., Sayyed, M. I., Tekin, H. O., Kaky, K. M., Baki, S. O., & Kityk, I. (2019). An Investigation on shielding properties of Bao, MoO₃ and P₂O₅ based glasses using MCNPX code. *Results in Physics*, 12, p. 629-634, 2019. <https://doi.org/10.1016/j.rinp.2018.12.003>

Biography

Elisha Daniel Edmund completed his Masters of Philosophy in Nuclear Science and Technology (Health Physics and Radiation Protection) from the University of Ghana in 2021. This work is a part of thesis submitted in fulfilment of the requirements of Masters of Philosophy in Nuclear Science and Technology at the University of Ghana. Since 2018 is employed by Tanzania Atomic Energy Commission (TAEC) as a Radiation Health Physicist.